Journal of Applied Mechanics and Technical Physics, Vol. 51, No. 4, pp. 521–528, 2010

SKIP TRAJECTORY FLIGHT OF A RAMJET-POWERED HYPERSONIC VEHICLE

V. M. Fomin, S. M. Aulchenko, and V. I. Zvegintsev

UDC 629.7.015

Possible skip trajectories of a flying vehicle with a periodically actuated ramjet are numerically simulated. An optimal choice of ramjet actuation areas and duration is demonstrated to ensure the maximum flight range with a given amount of the fuel. The main advantage of skip trajectories is found to be a significant (by an order of magnitude) decrease in thermal loads on the flying vehicle.

Key words: *ramjet, lift-to-drag ratio, skip trajectory.*

Introduction. The problem of motion of a hypersonic flying vehicle with skip-skip-skip-bouncing from the Earth's atmosphere for the purpose of increasing the flight range was first considered by Zänger and Bredt in 1944 [1]. They proposed to accelerate an aircraft with a launch mass of 100 tons to a velocity of 6000 m/sec by a liquid-propellant motor, which would allow the aircraft to go up to 260 km. During the subsequent descent with a non-operating motor, a significant lift force was generated at the moment when the aircraft entered the atmosphere, and it started to move upward again (bouncing off from the atmosphere). The aircraft was expected to make 10 cycles with a gradually decreasing amplitude and to fly approximately 18,000 km [2]. Keldysh [3] indicated that the thrust characteristics of the liquid-propellant motor in Zänger's aircraft were overestimated, and proposed to use a combination of a ramjet and a liquid-propellant motor with realistic thrust values. According to the estimates of [3], hybrid propulsion could boost the aircraft to a velocity of 5000 m/sec, after which the skip-bouncing descent of the aircraft with a non-operating motor provided a flight range of 11,800 km. Keldysh [3] was the first one to note that the skip trajectory of atmospheric flight allows significant reduction of thermal loads on the aircraft structure.

The interest in using skip trajectories is still retained. Thus, Kiselev and Fetisov [4] proposed to use skip trajectories for intercontinental ballistic missiles moving with velocities up to 8000 m/sec in the range of altitudes $H = 100$–150 km, which allows the flight range to be increased to 10,000–15,000 km with an acceptable level of thermal loads. Khilkevich and Yanovskii [5] demonstrated that the use of bouncing can increase the flight range of surface-to-surface missiles by a factor of 1.5–2.2. Shumilin [6] reported some specific features of hypersonic flights over wavy trajectories, which were organized by specialists from the USA and China.

Possible skip trajectories of a flying vehicle with a periodically actuated ramjet are analyzed in the present paper. An optimal choice of motor actuation areas is demonstrated to ensure the maximum flight range for a given amount of the fuel.

Formulation of the Problem. As a typical hypersonic flying vehicle, we consider a two-stage surface-to-surface missile with a solid-propellant booster (solid-propellant rocket motor) as the first stage and a ramjet used for propulsion of the second (marching) stage. The launch mass of the missile was assumed to be 1000 kg. Based on statistical data, the missile with this mass was assumed to have a diameter of 500 mm. Depending on the calculation variant, the fuel necessary for the solid-propellant booster and ramjet was 30 to 90% of the launch mass. A sketch of the missile considered is illustrated in Fig. 1a; for comparison, Figs. 1b and 1c show the real configurations of anti-aircraft missiles with hybrid propulsion: ZUR 3M9 (a system called a Cube) and ZUR 17D, respectively [7].

Khristianovich Institute of Theoretical and Applied Mechanics, Siberian Division, Russian Academy of Sciences, Novosibirsk 630090; aultch@itam.nsc.ru. Translated from Prikladnaya Mekhanika i Tekhnicheskaya Fizika, Vol. 51, No. 4, pp. 85–94, July–August, 2010. Original article submitted June 27, 2009.

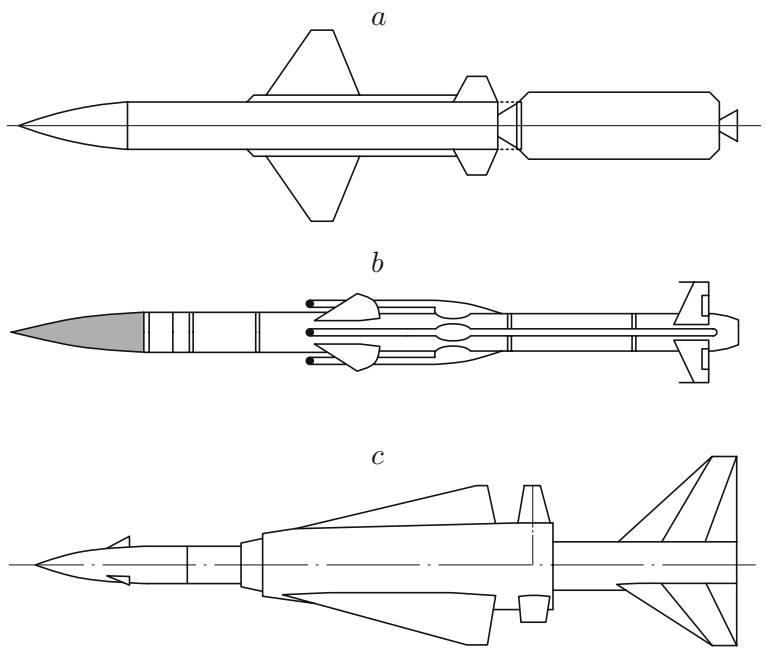

Fig. 1. Configurations of missiles with hybrid propulsion containing a solid-propellant booster and a ramjet: missile considered in the present work (a); real missile configurations ZUR 3M9 (b) and ZUR 17D (c).

TABLE 1

Calculated Specific Impulse of the Ramjet

M	I_{sp}						
	$H = 2$ km	$H = 5$ km	$H = 11$ km	$H = 25$ km	$H = 30$ km	$H = 35$ km	$H = 40$ km
3.0	11,300.0	11,493.0	11,848.0	11,729.0	11,554.0	11,363.0	11,000.0
3.5	11,492.0	11,760.0	12,322.0	12,230.0	11,969.0	11,700.0	11,430.0
4.0	11,338.0	11,610.0	12,253.0	12,176.0	11,870.0	11,563.0	11,258.0
4.5	10,926.0	11,302.0	12,018.0	11,925.0	11,592.0	11,251.0	10,914.0
5.0	10,322.0	10,704.0	11,511.0	11,423.0	11,053.0	10,687.0	10,321.0
5.5	9583.2	9984.9	10,858.0	10,744.0	10,348.0	9957.4	9568.3
6.0	9000.0	9200.7	10,105.0	9989.6	9568.6	9141.1	8729.9

Propulsion Parameters. The specific impulse of the ramjet was assumed to be constant: $I_{sp} = 2200$ m/sec. The solid-propellant booster operation time was determined from the specified mass and flow rate of the fuel necessary to ensure a constant thrust force exceeding the initial weight of the vehicle by a factor of 10.

The calculations of the thrust characteristics of the ramjet took into account the relative geometric parameters of the duct, the dependence of the atmospheric parameters on the altitude, the ratio of the fuel and oxidizer masses, and the real thermophysical properties of air and combustion products [8]. Kerosene was considered as a fuel, the design Mach number for the intake was M = 4, the area of the flow captured by the intake was equal to the missile mid-section area, the throat area could be varied, the air-to-fuel ratio was 1.0, the combustion efficiency was 0.95, and the losses in the nozzle were 0.95. Typical values of the ramjet specific impulse for different flight conditions are listed in Table 1. Depending on the altitude and flight Mach number, the thrust characteristics obtained for chosen geometric parameters were approximated by power polynomials, which were further used to speed up trajectory calculations. The law of ramjet control chosen for trajectory calculations implies that the fuel flow rate varies in proportion to the air mass flow through the intake; therefore, the air-to-fuel ratio remains constant during the entire period of ramjet operation.

Trajectory Calculations. The trajectory characteristics for each set of the parameters λ_i and t_i $(i = 1, \ldots, m)$, which define the actuation time λ_i and the duration of engine operation t_i, are found by solving a system of equations of motion of the flying vehicle in the vertical plane. With allowance for the drag and thrust forces in projections onto the axes of the flow-fitted coordinate system, the equations of motion in the field of the gravity force take the form [9, 10]

$$m\frac{dV}{dt} = P\cos(\alpha + \varphi_{\text{eng}}) - X - mg\sin\theta,$$
$$mV\frac{d\theta}{dt} = P\sin(\alpha + \varphi_{\text{eng}}) + Y - mg\cos\theta + m\frac{V^2\cos\theta}{R_{\text{Earth}} + H}, \tag{1}$$

where m is the variable mass of the vehicle, V is the flight velocity, t is the time, P is the propulsion (thrust force), X and Y are the drag and lift forces, respectively, θ is the slope of the flight trajectory, g is the free-fall acceleration, R_{Earth} is the Earth radius, H is the flight altitude, α is the angle of attack of the vehicle, and φ_{eng} is the angle of engine mounting with respect to the longitudinal axis of the vehicle. In our calculations, we assumed that $\alpha = \varphi_{\text{eng}} = 0$, and the direction of propulsion P coincides with the engine axis direction. The term $mV^2\cos\theta/(R_{\text{Earth}} + H)$ takes into account the change in the centripetal acceleration induced by the Earth surface curvature. To simplify the calculations, the drag coefficient was assumed to be constant in the entire range of flight velocities: $C_x = 0.3$. To perform bouncing maneuvering, the marching stage has special surfaces generating the lift force with a constant lift-to-drag ratio $K = Y/X = 1.5$–3.5.

The equations of motion (1) are supplemented with kinematic equations relating the flight range L and altitude H to the flight velocity and trajectory slope

$$\frac{dL}{dt} = \frac{dx}{dt} = V\cos\theta\frac{R_{\text{Earth}}}{R_{\text{Earth}} + H}, \qquad \frac{dH}{dt} = \frac{dy}{dt} = V\sin\theta, \tag{2}$$

and also the equation that describes the change in the flying vehicle mass due to fuel combustion

$$m(t) = m_0 - \int_0^t G_{\text{sec}}\,dt, \tag{3}$$

where G_{sec} is the flow rate of the fuel in one second and m_0 is the initial mass of the vehicle.

System (1)–(3) was integrated numerically by the second-order Runge–Kutta method with a constant time step. Each trajectory considered consists of three characteristic segments: boost segment, basic segment, and descent segment. The boost segment was ignored in calculating the flight range.

Boost Segment. The vehicle is launched owing to the thrust force generated by the solid-propellant booster from the surface at $H = 0$ and $V = 0$ with a certain initial trajectory angle θ_0. The rational value for our problem is $\theta_0 = 60$–$90°$. The solid-propellant booster operation time was determined from the specified fuel mass for the booster and the flow rate that ensured a constant thrust force exceeding the initial weight of the vehicle by a factor of 10. Typical flight trajectories on the boost segment are shown in Fig. 2. Figure 3 shows the variation of the flight velocity during climbing. It is seen that the vehicle is accelerated when the engine is in operation, and the flight velocity drastically decreases after the engine is switched off. It should be noted that the booster operation is finalized at a moderate altitude for a wide range of the initial conditions, and the further flight of the vehicle is determined to a large extent by the atmospheric drag. If hybrid propulsion is used for acceleration, then booster operation is followed (with a small delay of approximately 1 sec) by opening of an intake with a constant-area air stream captured by the intake, and the ramjet is actuated, which allows the vehicle to continue accelerating and climbing. It is seen from Figs. 2 and 3 that the use of hybrid propulsion allows the flight velocity and altitude to be substantially increased after the boost segment. Figure 4 shows the flight altitude and velocity ranges at the engine shutdown instant for different values of the fuel mass used for boosting. Different points correspond to different values of the launch angles. It is seen that vehicle acceleration to a velocity of 2000 m/sec by the solid-propellant booster requires the amount of the fuel greater than 70% of the launch mass of the vehicle. Acceleration to the same velocity with the use of hybrid propulsion requires the amount of the fuel within 40% of the launch mass.

Descent Segment. When the entire amount of the fuel is consumed, the missile starts descending with the engine switched off. The velocity and density of the incoming flow increase. If the lift-to-drag ratio is sufficiently

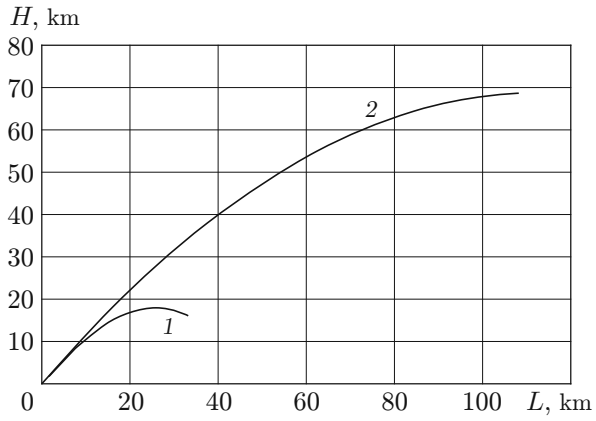

Fig. 2

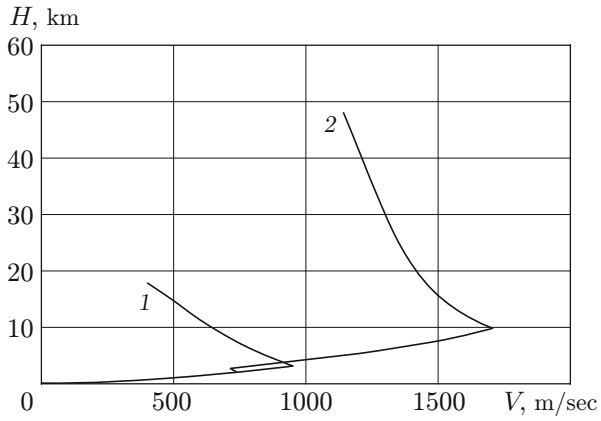

Fig. 3

Fig. 2. Typical trajectories of vehicle boosting with the solid-propellant booster (1) and with the solid-propellant booster combined with the ramjet (2).

Fig. 3. Flight velocity versus flight altitude during vehicle boosting (notation the same as in Fig. 2).

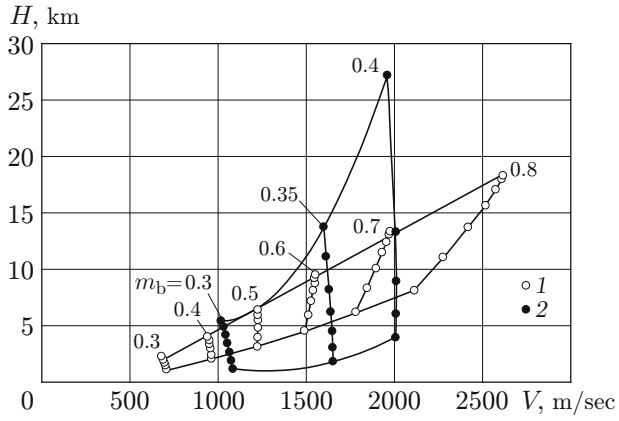

Fig. 4

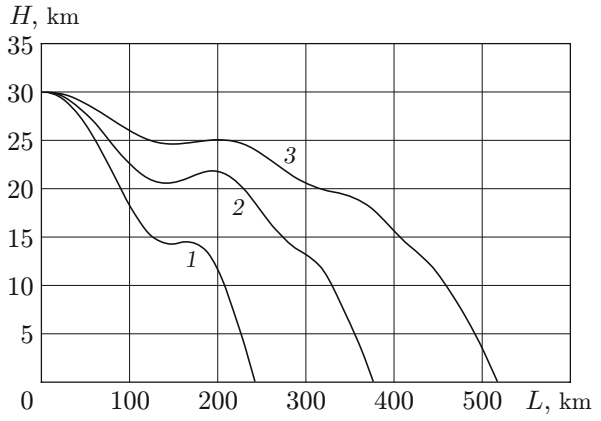

Fig. 5

Fig. 4. Flight conditions at the end of the boost segment: solid-propellant booster at $\theta_0 = 60$–90° (1) and solid-propellant booster with ramjet at $\theta_0 = 50$–70° (2); the numbers in the figure indicate the relative mass of the fuel m_b used for vehicle boosting.

Fig. 5. Gliding trajectories of the vehicle with a non-operating engine for $m = 600$ kg, $V_0 = 1500$ m/sec, $\theta_0 = 0^\circ$, and different values of the lift-to-drag ratio: $K = 1.5$ (1), 2.5 (2), and 3.5 (3).

high, the missile descent trajectory may have inflection points where the lift force balances the gravity force, and the missile starts ascending. The descent trajectory of the missile with a non-operating engine is shown in Fig. 5. It is seen that the missile performs a bouncing or gliding flight during a certain period (until its contact with the surface). The length of the descent segment depends on the missile mass, altitude, and velocity at the initial point and on the lift-to-drag ratio of the missile. In our calculations, the length of the descent segment was 5 to 20% of the length of the basic segment of the trajectory.

Basic Segment. Based on characteristics obtained on the boost segment, we assumed that the mass of the marching stage after its boosting is 60% of the total launch mass, and the flight velocity is 500 to 2500 m/sec in the range of altitudes from 5 to 50 km. In its further flight, the missile can follow one of the two qualitatively different trajectories considered below.

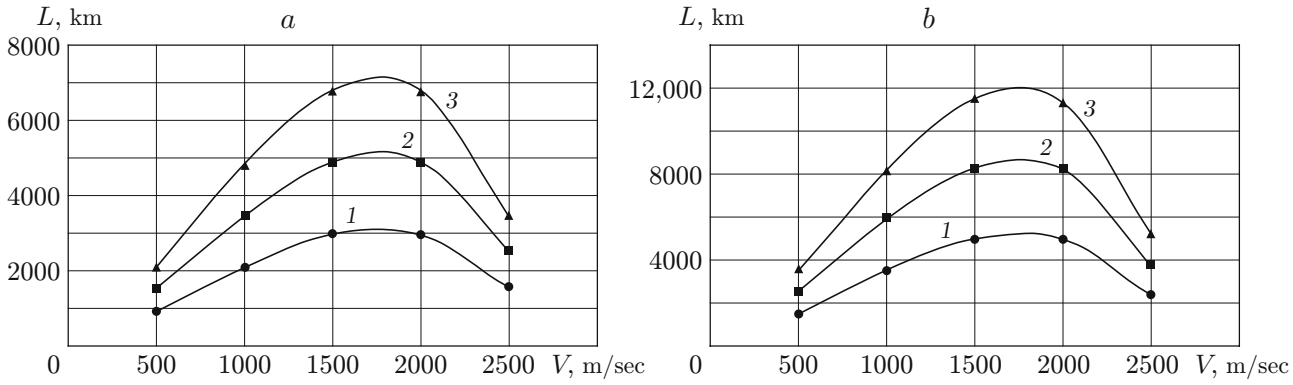

Fig. 6. Flight range of a ramjet-powered missile over a trajectory with constant parameters versus velocity for $H = 20$ km and $K = 1.5$ (1), 2.5 (2), and 3.5 (3): (a) $m_{\rm f} = 0.76m_0$; (b) $m_{\rm f} = 0.88m_0$.

Trajectory with Constant Parameters. Our primary goal was to solve the problem of a missile flying with an operating ramjet at a constant altitude with a constant velocity in the ranges of altitudes and velocities considered. To ensure such a flight, the lift force should be rigorously consistent with the vehicle weight, and the thrust force should correspond to the drag force. With the lift-to-drag ratio and the vehicle mass being specified, the necessary values of the thrust force and the flow rate of the fuel in the ramjet can be easily found. Note that the vehicle mass decreases as the fuel is gradually consumed, and it is necessary to control (decrease) the engine thrust to maintain a constant flight altitude and velocity. Because of the low atmosphere density at altitudes above 30 km, the ramjet intake area should be substantially increased; therefore, the constant-velocity flight at these altitudes was not considered.

The typical flight ranges over a trajectory with constant parameters are shown in Fig. 6. It is assumed that an identical amount of the fuel (40%) is consumed at the boost segment before a chosen altitude and velocity are reached, whereas the remaining 36% (Fig. 6a) or 48% (Fig. 6b) of the launch mass of the flying vehicle are consumed on the marching segment. It is seen that the flight range is substantially affected by the lift-to-drag ratio. The optimal flight velocity is 1500–2000 m/sec (Mach number M = 5–7). With the maximum value of the lift-to-drag ratio ($K = 3.5$) and the available amount of the fuel onboard equal to 88% of the initial mass of the vehicle, the flight range can reach 12,000 km (with allowance for the descent segment whose length is 3–6% of the marching segment length).

It is of interest to compare the calculated results with real data obtained in the flight of the Burya intercontinental cruise missile, which was tested in the USSR in 1957–1960 [11]. The launch mass of this cruise missile was 98,280 kg. The missile was boosted to the altitude $H = 18$ km and velocity $V = 915$ m/sec (M = 3.1) by two jettisoned liquid-propellant boosters with the total mass of 64,760 kg, and the amount of the fuel allocated for boosting was 54,280 kg (55% of m_0). The marching stage had a mass of 33,520 kg, with the amount of kerosene for ramjet operation 27,200 kg (28% of m_0). The Mach number on the basic segment of the flight trajectory was constant (M = 3.1–3.2) with a small increase in the altitude from 17.5 to 25.5 km. The flight range of the Burya cruise missile was expected to be 8000 km, and the real flight range was 6500 km. The characteristics available for this missile are in good agreement with the estimates calculated in the present work (curve 3 in Fig. 6b).

Despite successful test results, the Burya intercontinental cruise missile was not commissioned because of the realistic (even in the 1960s) possibility of capturing the marching stage during its long-time straight-line flight.

Skip Trajectory. As was demonstrated above, the use of the lift-to-drag ratio effect even without propulsion allows the vehicle to fly over a skip trajectory and, thus, substantially increase its flight range. The main idea of this work was to use a combination of the lift-to-drag ratio and periodic actuation of the ramjet in order to ensure a long-time bouncing flight. The optimization approach was used for the rational choice of the time instants T_i of engine actuation and shutdown.

The optimization problem is formulated in the general form as follows. We have to find $\min \Phi(x)$ $(x \in X)$ under the conditions

$$E_m \supset X = \{x: \quad x_i' \leqslant x_i \leqslant x_i''\}, \qquad i = 1, \ldots, m,$$

$$\varphi_j(x) = 0, \quad j = 1, \ldots, N, \qquad \psi_j(x) \leqslant 0, \quad j = 1, \ldots, N'.$$

The composite functional has the form

$$\Phi_{\text{comp}} = \Phi_0\Big[\sum_{j=1}^{N} k_j\Big(\frac{\varphi_j}{\varepsilon_j}\Big)^2 + \sum_{j=1}^{N'} k'_j\Big(\frac{\psi_j}{\varepsilon'_j} + \Big|\frac{\psi_j}{\varepsilon'_j}\Big|\Big)^2 + 1\Big].$$

Here, $\Phi_0 = (1 + \Phi)$ (Φ is the objective functional), ε and ε' are the specified values of accuracy with which the constraints have to be satisfied, and k and k' are the penalty coefficients whose initial values are specified and then refined in the course of program operation.

In the problem considered, we have $\Phi(x) = 1/L(x)$, where $L(x)$ is the distance between the initial and final trajectory points. The set of optimization parameters consists of the subset of parameters $0 < \lambda_i < 1$ $(i = 1, \ldots, m)$ and the subset of parameters $0 < t_i < t_d$ $(i = 1, \ldots, m)$. Based on the transformation

$$T_i = T_{i-1} + (T_{i-1} - T_{i-2})\Big(\frac{1}{\lambda_{i-1}} - 1\Big), \quad i = 2, \ldots, m-1, \qquad T_1 = T_0 + \frac{T_m - T_0}{S_{m-1}},$$

where

$$T_0 = 0, \quad T_m = T_k, \quad S_1 = 1, \quad S_i = S_{i-1}\Big(\frac{1}{\lambda_i} - 1\Big) + 1, \quad i = 1, \ldots, m-1,$$

the parameters λ_i define a monotonic distribution of the time instants T_i of engine actuation. By varying λ_i, it is possible to specify any desired distribution of T_i. The parameters t_i define the time of engine operation after each actuation. Using functional constraints, one can define, for example, the minimum value of the vehicle "dipping." It is also possible to solve optimization problems in different formulations, for instance, to determine the minimum amount of the fuel necessary to cover a specified distance, etc.

The solution of the optimization problem proper reduces to solving the problem of minimization of a function of numerous variables. The minimization method used in this work, which can be characterized as a gradientless method of searching with adaptation and the use of a random element, was implemented as a specialized set of programs synthesized on the basis of modified methods of rotating coordinates, direction cosine, and matrix descent [12].

The initial data used in the calculations were also the vehicle mass, the flight velocity and altitude after vehicle boosting, and the constant value of the lift-to-drag ratio. The angle of the trajectory slope at the beginning of the basic segment was usually assumed to be $\theta = 0°$. With the use of the optimization program, the instants of engine actuation and the ramjet operation duration were varied to obtain the maximum flight range. The changes in propulsion characteristics depending on the flight altitude and velocity were taken into account. A typical skip trajectory of a flying vehicle with a periodically actuated ramjet is shown in Fig. 7. In the case considered, the total flight range was 6000 km, and the flight duration was 4217 sec. The engine was switched on 15 times and was in operation for a total of 1276 sec.

Figure 8 shows the time evolution of the flight altitude, flight velocity, and slope of the flight trajectory at the initial part of the flight. The flight velocity is seen to increase approximately to 1500 m/sec owing to trajectory oscillations, The mean horizontal flight velocity is 6000 km/4217 sec = 1423 m/sec. The trajectory slope changes in the interval $-10° < \theta < 10°$.

Typical flight ranges for the case of motion of a ramjet-powered vehicle over a skip trajectory are shown in Fig. 9. As previously, it is assumed that an identical amount of the fuel (40%) is consumed at the boost segment until the chosen flight altitude and velocity are reached, whereas the remaining 36% (see Fig. 9a) or 48% (see Fig. 9b) of the launch mass of the vehicle are consumed on the marching segment.

With the maximum value of the lift-to-drag ratio ($K = 3.5$) and the available amount of the fuel onboard equal to 88% of the initial mass of the vehicle, the flight range over the skip trajectory can reach 11,000 km (with allowance for the descent segment). Comparing the data for skip trajectories (see Fig. 9) with the results for trajectories with a constant flight velocity (see Fig. 6), we can note that there are no significant differences in the maximum flight ranges reached. A significant increase in the flight range at high (above 2000 m/sec) and low (below 1000 m/sec) initial flight velocities should be noted. In those cases, owing to periodic actuation of the ramjet, the mean flight velocity is leveled off at approximately 1500 m/sec.

The main advantage of the flight over a skip trajectory is a significant decrease in the level of aerodynamic heating of the flying vehicle. It is known that the integral of $\rho V^3/2$ (ρ is the mass density of air) with respect

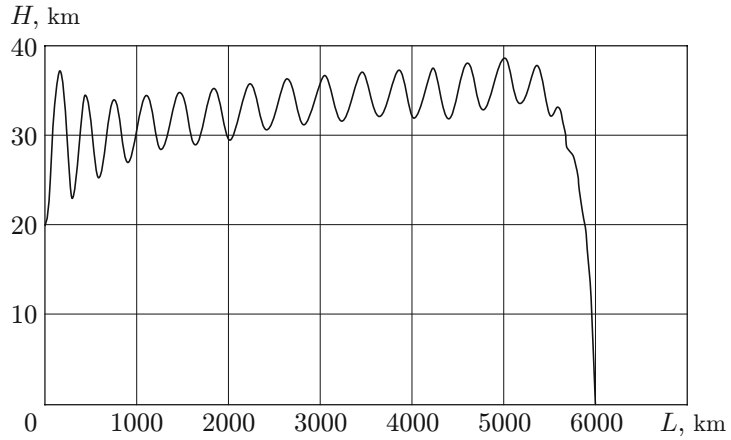

Fig. 7. Basic segment and descent segment of the skip trajectory of a ramjet-powered vehicle for $H_0 = 20$ km, $V_0 = 1000$ m/sec, $m_0 = 600$ kg, $\theta_0 = 0^\circ$, and $K = 3.5$ at the beginning of the basic segment.

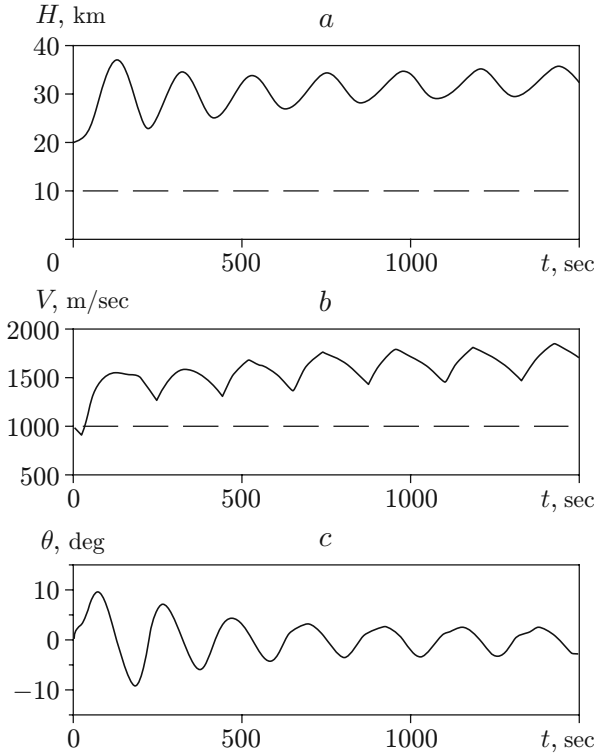

Fig. 8

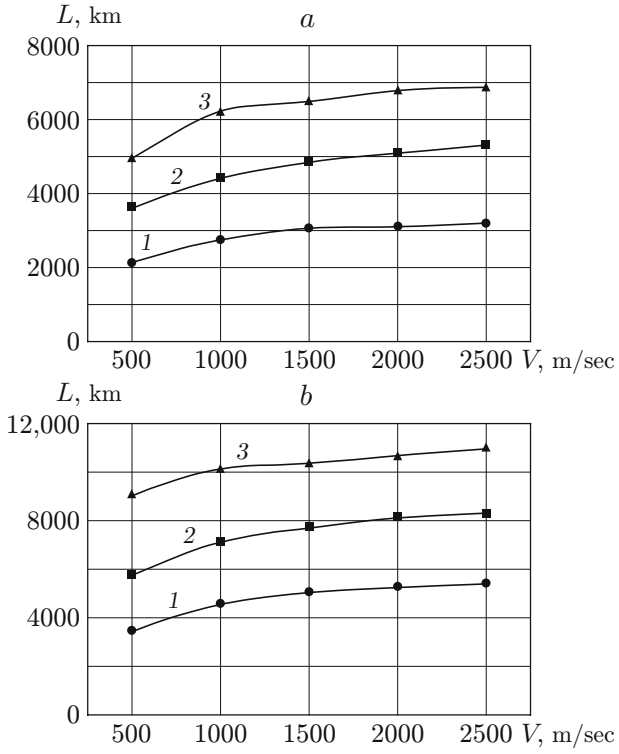

Fig. 9

Fig. 8. Characteristics of the vehicle flight over the initial part of the trajectory shown in Fig. 7: (a) altitude; (b) velocity; (c) trajectory slope; the horizontal bars indicate the engine operation time.

Fig. 9. Flight range of a ramjet-powered vehicle over the skip trajectory versus velocity (notation the same as in Fig. 6).

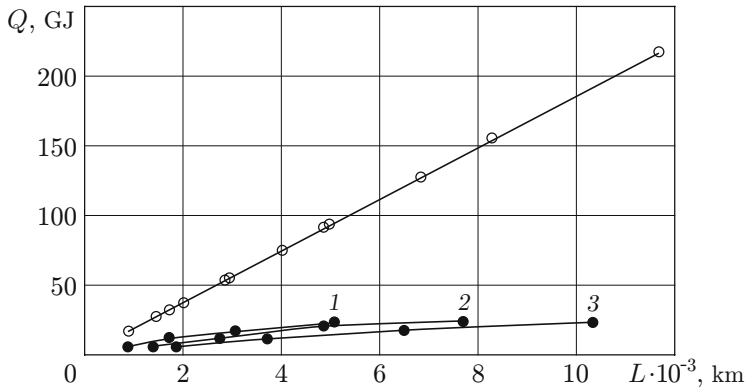

Fig. 10. Amount of heat acting on the vehicle during its flight versus the flight range: the open and filled points are the results for the constant-velocity flight and for the flight over the skip trajectory with the lift-to-drag ratio being $K = 1.5$ (1), 2.5 (2), and 3.5 (3).

to time can be considered as the upper limit of the amount of heat Q acting on the vehicle during its flight (see, e.g., [13]). The amount of heat is plotted in Fig. 10 as a function of the flight range for the trajectory variants considered. It is seen that the bouncing effect allows the amount of heat acting on the vehicle to be reduced by an order of magnitude.

Conclusions. The theoretical study performed demonstrated the prospects of using ramjet-powered flying vehicles to obtain the flight range of 7000–11,000 km with the amount of the fuel onboard up to 76–88% of the initial mass of the vehicle. The flight range of the vehicle over a skip trajectory with periodic actuation of the ramjet differs only slightly from the flight range of the vehicle with a continuously operating engine. The main advantage of using skip trajectories is a significant (by an order of magnitude) decrease in thermal loads acting on the vehicle.

REFERENCES

1. E. Zänger and I. Bredt, *Long-Range Bomber with a Rocket Motor: Review of Captured Equipment* [Russian translation], Voenizdat, Moscow (1946).
2. W. Ley, *Rockets, Missiles, and Space Travel*, Viking, New York (1961).
3. M. V. Keldysh, *Selected Papers. Rocket and Space Engineering* [in Russian], Nauka, Moscow (1988).
4. V. I. Kiselev and V. A. Fetisov, "Method of controlling a hypersonic flying vehicle," RF Patent No. 2167794, MPK V 64 G 1/62, Publ. 02.21.2000, Byul. Izobr. Polez. Modeli, No. 15, Part 2.
5. V. Ya. Khilkevich and L. S. Yanovskii, "Application of bouncing and pitching effects for increasing the flight range of missiles," *Izv. Vyssh. Uch. Zaved., Aviats. Tekhnika*, No. 3, 70–72 (2005).
6. A. Shumilin, "Hypersonic long-range bombers may appear in the USA in 30 years," URL: http://nvo.ng.ru/armament/2000-08-18/6_avia.html.
7. V. N. Aleksandrov, V. M. Bytskevich, V. K. Verkholomov, et al., *Integral Solid-Propellant Air-Breathing Engines* [in Russian], Akademkniga, Moscow (2006).
8. V. M. Fomin, V. I. Zvegintsev, I. I. Mazhul, and V. V. Shumskii, "Comparison of the energy capabilities of ramjets and solid-propellant boosters in terms of propulsion for boosting small-scale flying vehicles," *J. Appl. Mech. Tech. Phys.* (in press).
9. A. A. Lebedev and L. S. Chernobrovkin, *Flight Dynamics of Unmanned Flying Vehicles* [in Russian], Oborongiz, Moscow (1962).
10. I. V. Ostoslavskii and I. V. Strazheva, *Flight Dynamics. Trajectories of Flying Vehicles* [in Russian], Mashinostroenie, Moscow (1969).
11. M. D. Evstaf'ev, *Long Way to Burya* [in Russian], Vuz. Kniga, Moscow (1999).
12. A. F. Latypov and Yu. V. Nikulichev, "Specialized complex of optimization programs," Preprint No. 15-85, Inst. Theor. Appl. Mech., Sib. Div., Acad. of Sci. of the USSR, Novosibirsk (1985).
13. A. N. Ponomarev, *Years of the Space Era* [in Russian], Voenizdat, Moscow (1974).